2009 American Control Conference
Hyatt Regency Riverfront, St. Louis, MO, USA
June 10-12, 2009

Robust Engine Torque Control by Iterative Learning Control

Takashi Nagata and Masayoshi Tomizuka

***Abstract*—Fast-response engine torque control is robustly realized under repetitive air throttle input. An application of iterative learning control (ILC) to robustify the performance of disturbance observer (DOB) is proposed and numerically evaluated. The proposed scheme detects dynamical model discrepancy between an actual engine and its nominal model, and compensate for it to realize nominal plant dynamics. With the applied ILC realizing improved detection of model discrepancy, the scheme is significantly more effective than a conventional DOB under practical test-bench conditions such as measurement delays, noise, and insufficient data measurements.**

I. Introduction

Torque based control is in high demand in modern automotive powertrain applications. When driving a car, it is expected that there is a high occurrence of repeated engine torque manipulations as seen in gas pedaling maneuvers over iterative vehicle start-up's and transmission gear shiftings. Torque control performance can improve significantly if the iterative nature can be utilized in the controller design.

An important application of engine torque control is smooth gear shifting. A previous study [1] presented a collaborative scheme between engine control and automatic transmission (AT) gearbox control. For a given gear shifting from a certain gear position to another in a conventional automatic transmission gearbox, one can obtain an engine torque reference profile for the engine torque controller as well as hydraulic actuations reference profiles for the AT gearbox controller. By each individual controller conducting its own tracking control with respect to individually provided reference profiles, smooth torque and speed controls are realized at the wheel so that the driver and passengers feel no abrupt changes in acceleration from longitudinal motion.

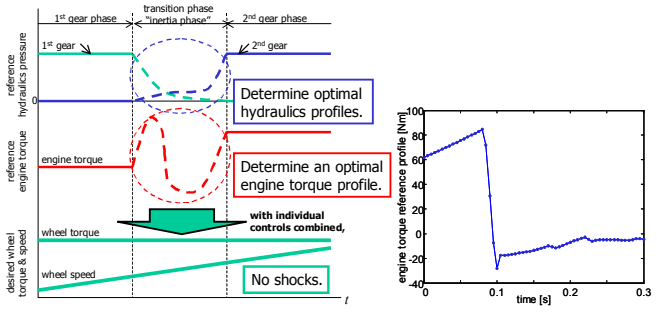

Fig. 1. Smooth gear shifting by engine / AT collaboration.

Research is supported by Toyota Motor Corporation. The authors would like to thank Mr. Akira Ohata, Mr. Junichi Kako, Dr. Tomoyuki Kaga and Mr. Noriyasu Adachi of Toyota for valuable technical discussions.

The authors are with the Department of Mechanical Engineering, University of California, Berkeley, CA 94720-1740 (e-mails: (Nagata) taka_me@newton.berkeley.edu, (Tomizuka) tomizuka@me.berkeley.edu).

An example of engine torque reference profile for 1st-to-2nd gear shifting is shown in Fig. 1. The profile prescribes engine torque generation over a short duration in the order of 100ms since a short duration is preferred for gear shifting. This highlights the need for engine torque tracking with a sufficiently fast response. Therefore, a model-based approach is essential for this purpose.

Direct and fast-response measurement of engine torque has become available by in-cylinder pressure sensors [2]. The gross engine torque generated inside a cylinder, also known as indicated torque, is obtained by numerically integrating the measured in-cylinder pressures in real time. Discrete event engine models [3] have also been applied to control engine torque. Nagata and Tomizuka examined disturbance observer to achieve robust stability and performance of the torque generation process by adjusting the throttle air intake [4],[5].

While existing schemes by disturbance observers (DOB) can handle the model discrepancy between the actual and nominal plants as equivalent input disturbance, the resulting characteristics of a standard DOB is prone to deviate from desired nominal characteristics. This deviation can be caused by delay (dead time) in the engine from its input to output, and insufficient data measurements and coarse data interpolations as will be presented in this paper. Since the standard DOB does not remember its own past actions, the resulting deviations will be repeated in the same manner if repeated control cycles are assumed. Furthermore, the problems from delay and inadequate data interpolation cannot be fundamentally addressed as long as the controller structure remains causal, which is the case for standard DOB's.

Iterative learning control (ILC)[6] holds a key in addressing these problems since it takes advantage of repetitiveness by learning from previous error transients across repetition cycles as well as by allowing for acausal design in learning from future errors within one control cycle. This study explores a combination of DOB and ILC, and also evaluates the effects of non-repetitiveness in the proposed scheme.

II. Engine Torque Control Strategy with a Conventional Disturbance Observer Scheme

A. Multi-input scheme for fast-response control

The engine model under study assumes two inputs and one output (Fig. 2). The inputs are the air mass intake adjusted at the throttle (or "air though throttle") m_{at}, and the fuel injection adjustment m_{fi}. The output is the generated torque T_{gen}. These are discrete signal sequences whose discretization step is 180 deg. in crankshaft increment i.e. a combustion stroke.

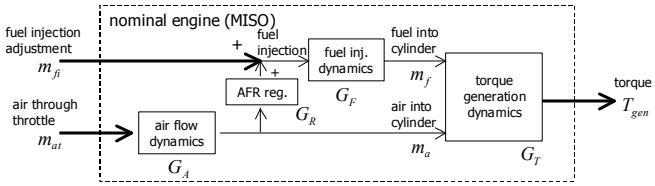

Fig. 2. Multi-input engine model.

The model consists of component dynamics i.e. air flow dynamics G_A, fuel injection dynamics G_F, torque generation dynamics G_T, and air-to-fuel (AFR) regulator dynamics G_R. These are discrete event models as described in [4],[5]. In this study, the multi-input scheme has a newly introduced input m_{fi} independent of m_{at} that together affect the output T_{gen}.

$$T_{gen} = G\begin{bmatrix} m_{fi} \\ m_{at} \end{bmatrix} \text{ where } G = \begin{bmatrix} G_{Tf} & G_{Ta} \end{bmatrix} \quad \begin{aligned} G_{Tf} &= G_T G_F \\ G_{Ta} &= G_T G_F G_R G_A \end{aligned} \quad (1)$$

$$G_A(z) = \frac{\frac{X}{1+X} z}{z - \frac{1}{1+X}} \qquad G_F(z) = (1-K) + K\frac{1-F}{z^4 - F}$$

$$G_R(z) = \frac{1}{14.7} \qquad G_T(z) = z^{-d}\frac{H_u}{\pi}\eta_i$$

X is a parameter related to the volumetric efficiency η_{vol}. For a 4 cylinder engine, $X = \eta_{vol}(\omega_e, P_{man}) \times {}^{V_d}\!/_{4V_{man}}$ where P_{man} is the intake manifold pressure, V_d is the engine displacement, and V_{man} is the volume of the intake manifold. F is a parameter related to the fuel evaporation time constant τ_f, and it also depends on the engine speed ω_e as $F = \exp(-{}^{4\pi}\!/_{\omega_e \tau_f})$. K is a fuel adhesion parameter representing the rate of injected fuel deposited inside intake port prior to cylinder, hence $0 \le K \le 1$. H_u is the specific enthalpy of fuel, η_i is the thermal efficiency of the engine. z^{-d} represents the combustion delay from fuel injection during the intake stroke. $d = 2$ is therefore assumed.

As a motivation for having an independent fuel input, we note that fuel injectors can easily manipulate fuel input on a stroke-by-stroke basis, which allows the plant to exhibit a faster torque response than having the air throttle as the sole input. Conversely, it can be stated that a more lenient requirement is permissible for the throttle actuator whose bandwidth limitation is often a bottleneck in realizing fast-response torque control.

On fuel injection adjustment, the AFR regulator (see Fig. 2) determines the amount of fuel injection for steady state. Engine can run even when $m_{fi} = 0$ since this case corresponds to a single-input scheme studied in [4],[5]. This means the fuel injection adjustment m_{fi} is supplementary in nature and helps realizing short transient i.e. high frequency torque control.

B. *Use of the multi-input scheme for disturbance observer*

In practical model-based controls, one must compensate for model discrepancies between the actual plant and the nominal model in order to achieve both stability and performance. Disturbance observers (DOB) handle this issue by detecting the model discrepancy as an equivalent input disturbance, and subsequently canceling it by a negative feedback of the estimated equivalent input disturbance.

1) *Fuel disturbance observer (fuel DOB)*

In conjunction with the fuel injection adjustment m_{fi}, it is possible to design a disturbance observer based on m_{fi} rather than air intake through throttle m_{at}. It is assumed that this fuel input based DOB (fuel DOB) complies better with the actual physical nature of the engine, since most significant model uncertainties are expected to lie in high frequencies, and high frequency region is where fuel dynamics mainly takes place.

The equivalent fuel injection disturbance is estimated as $\hat{\tilde{m}}_{fi}$ below. z^{-2} is applied to resolve acausality in $G_{tf}^{-1} = G_F^{-1} G_T^{-1}$.

$$T_{gen} = G_{Tf}\tilde{m}_{fi} + G_{Ta}m_{at} \Rightarrow \hat{\tilde{m}}_{fi} = z^{-2}G_{Tf}^{-1}T_{gen} - z^{-2}G_{Tf}^{-1}G_{Ta}m_{at} \quad (2)$$

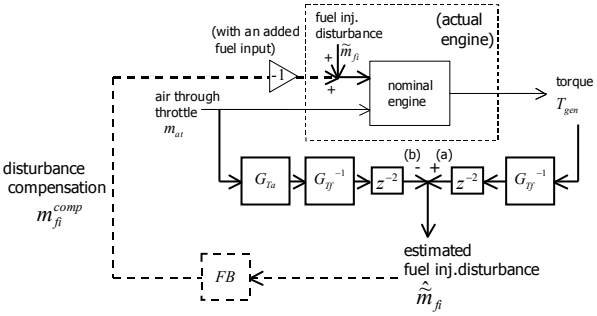

Fig. 3. Fuel DOB structure.

By deriving disturbance compensation m_{fi}^{comp} from $\hat{\tilde{m}}_{fi}$, nominal plant behavior from m_{at} to T_{gen} can be realized. The fuel DOB structure is suitable in addressing fuel related model uncertainties such as those in fuel injection dynamics and in AFR regulator dynamics. This is because the cause of model discrepancy is regarded as fuel injection disturbance which is more direct than air disturbance considered in [4],[5].

2) *Experimental results of the fuel DOB*

Fig. 4 shows the actual engine torque output T_{gen} measured after a stepwise throttle angle input. The horizontal axis is an index k to denote every 180 deg. crankshaft increment which corresponds to each stroke of the engine process. Nominal engine torque output $G_{Ta}m_{at}$ is also shown. The actual engine torque has shown larger than the nominal output in this case.

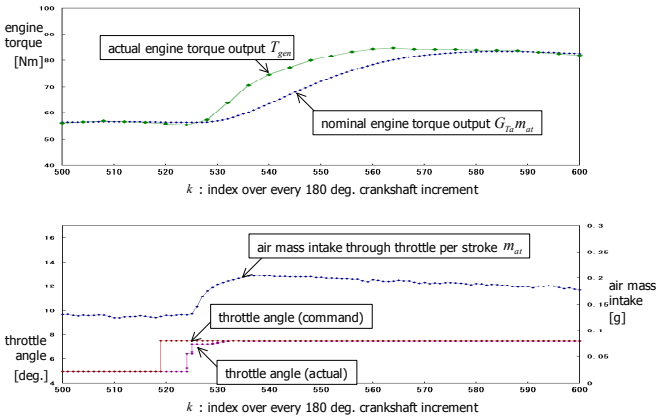

Fig. 4. Measurements from a step increase in throttle angle.

Fig. 5 shows an equivalent fuel injection $G_{Tf}^{-1}T_{gen}$ computed

from the actual output torque T_{gen}, and $G_{Tf}^{-1}G_{Ta}m_{at}$ which is another hypothetical fuel injection corresponding to the nominal output $G_{Ta}m_{at}$. Estimated equivalent fuel injection disturbance $\hat{\tilde{m}}_{fi}$ is obtained as their difference.

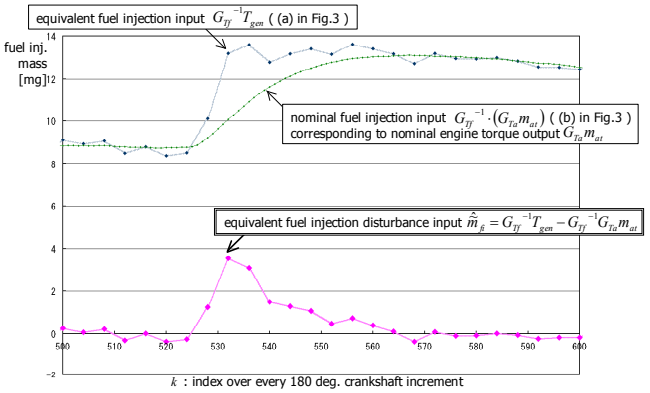

Fig. 5. Estimated equivalent fuel injection disturbance $\hat{\tilde{m}}_{fi}$.

It is, however, noted that $\hat{\tilde{m}}_{fi}$ is obtained only at every 4 stroke steps since the actual torque is measured only at every 4 stroke steps due to hardware limitations in the actual test-bench. This means that an interpolation scheme is required to obtain disturbance compensation m_{fi}^{comp} which must be defined at every stroke step for feedback control.

3) Model discrepancy compensation

Model discrepancy compensation is tested by simulation based on actual measurements (Fig. 6). The simulation assumes that the actual fuel injection disturbance is $\tilde{m}_{fi}$ = (linearly interpolated $\hat{\tilde{m}}_{fi}$ in Fig. 5), and disturbance compensation is m_{fi}^{comp} = ($\hat{\tilde{m}}_{fi}$ with zero order hold).

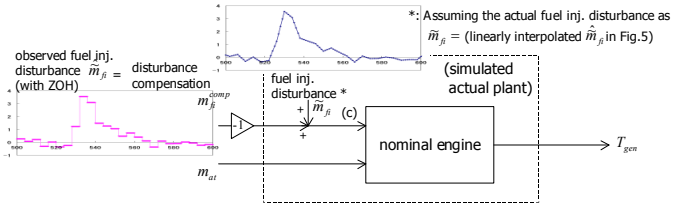

Fig. 6. Model discrepancy compensation by the conventional fuel DOB.

Fig. 7 shows the fuel input ((c) in Fig. 6) before and after applying m_{fi}^{comp}.

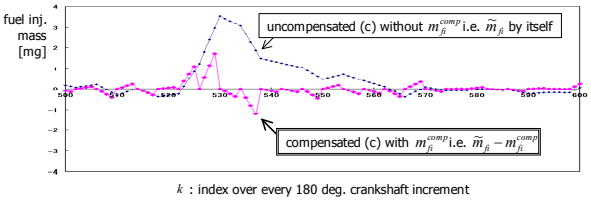

Fig. 7. Fuel input with and without disturbance compensation m_{fi}^{comp}.

It is shown that even after applying m_{fi}^{comp}, the fuel injection disturbance $\tilde{m}_{fi}$ is not completely cancelled out, due to the mismatch between the actual fuel injection disturbance $\tilde{m}_{fi}$ and the disturbance compensation m_{fi}^{comp}.

Fig. 8 shows the uncompensated engine torque from $\tilde{m}_{fi}$ which corresponds to the actual output torque, and also the compensated engine torque computed with $\tilde{m}_{fi}$ - m_{fi}^{comp}. The nominal engine torque $G_{Ta}m_{at}$ is also shown for reference.

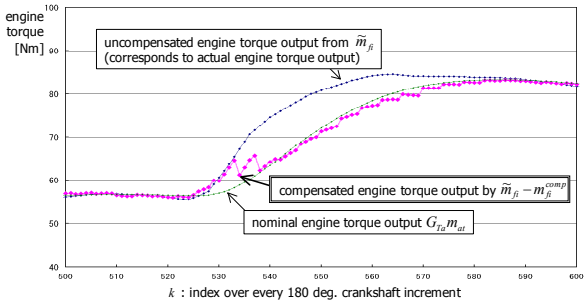

Fig. 8. Compensated engine torque with m_{fi}^{comp} and etc.

It is noted that the compensated torque output deviates largely from nominal torque output during the onset of torque increase i.e. k = 520 ~ 540. Also, after k = 540, the compensated output follows the nominal output with step-wise jitters. These trends are presumably due to the following inadequacies in the feed-backed disturbance compensation m_{fi}^{comp}; (a) delay from fuel injection timing to torque measurement (two strokes), and (b) insufficient torque data measurements and consequent coarse interpolation (each torque data is obtained only at every 4 stroke steps).

III. INTRODUCING ITERATIVE LEARNING TO FUEL DOB

A. Breaking the causality barrier

The objective of the fuel DOB discussed in the previous section is to know the equivalent fuel injection disturbance $\tilde{m}_{fi}$ accurately first, and then compensate for it by applying disturbance compensation m_{fi}^{comp} that essentially constitutes a negative feedback of $\tilde{m}_{fi}$. This realizes the nominal plant behavior from m_{at} to T_{gen}. However, conventional DOB schemes cannot appropriately handle delayed measurements and inadequate interpolation of insufficient data as shown in the previous section. These problems are inherently due to causality, therefore in order to resolve these issues, a new methodology is required that can allow for acausal designs.

Iterative learning control (ILC) [6] is one approach that can be useful. ILC is effective in rejecting repetitive disturbance when control is repetitive. In automotive powertrain control, it is expected that there is a high occurrence of repeated engine torque manipulations. For example, a course of car driving has iterative instances of vehicle start-up and transmission gear shifting that involve similar gas pedaling maneuvers for each instance. Therefore, ILC is expected to significantly improve torque control performance by utilizing in the controller design the iterative nature of the control as mentioned above. Based on this idea, the following scheme is developed to effectively realize an acausal smoothing of $\hat{\tilde{m}}_{fi}$ in Fig. 5, thus obtaining a far more improved estimate of $\tilde{m}_{fi}$.

B. *Application of iterative learning control (ILC)*

1) *ILC framework for the fuel DOB problem*

It is assumed that the air input m_{at} is a repetitive signal sequence. Then the output T_{gen} is also repetitive, meaning that the model discrepancy, represented by $\tilde{m}_{fi}$ i.e. the disturbance causing the difference between the actual output torque and the nominal engine torque output, should also be repetitive. Under these conditions, a control cycle (iteration) has length N. It is aimed that $m_{fi}^{comp}(j) = \{m_{fi,k}^{comp}(j)\}_{k=0}^{N-1}$, the disturbance compensation signal sequence obtained at j-th iteration, has a bounded limit $m_{fi}^{comp}(j \to \infty)$ matching $\tilde{m}_{fi} = \{\tilde{m}_{fi,k}\}_{k=0}^{N-1}$. For $\hat{\tilde{m}}_{fi}(j) = \{\hat{\tilde{m}}_{fi,k}(j)\}_{k=0}^{N-1}$, it should converge to $\hat{\tilde{m}}_{fi}(\infty) = \{0\}_{k=0}^{N-1}$ monotonically to realize nominal plant behavior accurately. Fig. 9 shows the ILC framework applied to the fuel DOB.

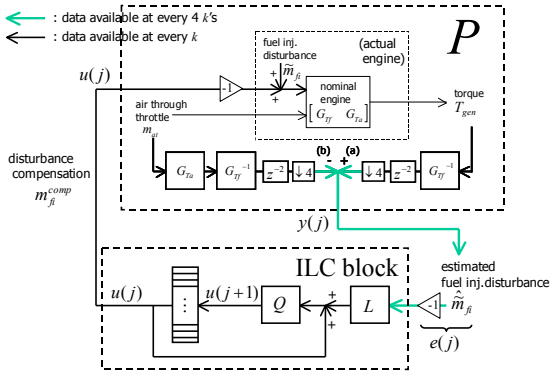

Fig. 9. ILC framework for the fuel DOB problem.

The plant P in the ILC framework has a delay z^{-2} and a down-sampler by 4 i.e. $\{\downarrow 4\}$ to reflect the two strokes delay and insufficient torque measurements. The plant dynamics is

$$y(j) = Pu(j) + d \tag{3}$$

where $y(j) = \hat{\tilde{m}}_{fi}(j)$ and $u(j) = m_{fi}^{comp}(j)$. It is noted that while the input $u(j)$ has length N, the output $y(j)$ has only length $N/4$. This means that the plant P is of size $N/4$ x N, not square. For the ILC block, the dynamics of $u(j)$ in the iteration direction is

$$u(j+1) = Q(u(j) + Le(j)) \tag{4}$$

where Q is a low pass filter with dynamics in the stroke steps i.e. k direction. Here, $w = Q(v)$ represents $w_k = \Sigma_{k'} q_{k-k'} v_{k'}$ with $w = \{w_k\}_k$, $v = \{v_k\}_k$, and $\{q_k\}_k$ is the unit pulse response of Q. L is a learning gain and will be explained later. $e(j)$ is the learning input to the ILC block and is represented by

$$e(j) = y_d - y(j) \;\Rightarrow\; e(j) = -y(j) = -\hat{\tilde{m}}_{fi}(j) \tag{5}$$

y_d is the desired trajectory for y. y_d is $\{0\}_{k=0}^{N-1}$ since $y(j) = \hat{\tilde{m}}_{fi}(j)$ and it is aimed that $\hat{\tilde{m}}_{fi}(j) \downarrow \hat{\tilde{m}}_{fi}(\infty)$ with $\hat{\tilde{m}}_{fi}(\infty) = \{0\}_{k=0}^{N-1}$. $e(j)$ has length $N/4$, hence the learning gain L is of size N x $N/4$.

It is stressed that both Q and L can be selected as acausal processes in the stroke steps i.e. k direction since all signals are available at any k as j progresses. This enables smoother data interpolation and delay cancellation within each iteration.

2) *On plant P for the ILC framework*

For application to the general ILC framework stated above, the exact expression of plant P for ILC is obtained as follows. Note that the air through throttle m_{at} (embedded inside P and not an input of P) does not affect $\hat{\tilde{m}}_{fi}$ since the signals from m_{at} cancel out at (a) and (b) in Fig. 9. Hence, the output $y(j) = \hat{\tilde{m}}_{fi}$ is connected only to signals $u(j) = m_{fi}^{comp}$ and $\tilde{m}_{fi}$ as

$$\begin{aligned}\hat{\tilde{m}}_{fi} &= \{\downarrow 4\}z^{-2}G_{Tf}^{-1}G_{Tf}\left(-m_{fi}^{comp} + \tilde{m}_{fi}\right) \\ &= -\{\downarrow 4\}z^{-2}m_{fi}^{comp} + \{\downarrow 4\}z^{-2}\tilde{m}_{fi}\end{aligned} \tag{6}$$

By comparing above expression with Eqn. (3), it is clear that

$$P = -\{\downarrow 4\}z^{-2},\; d = \{\downarrow 4\}z^{-2}\tilde{m}_{fi} \tag{7}$$

i.e. the plant P consists merely of a delay and a down-sampler.

3) *Choice of learning gain L*

The learning gain L prescribes the learning speed and is thus a design parameter when constructing an ILC scheme. In a general setting of ILC, it is preferred that the learning gain L equals to the inverse of the plant P i.e. $L = P^{-1}$ since this is known to realize dead-beat learning in which learning converges in just one iteration step. However, this is not possible in the current fuel DOB application since the plant P for ILC is not square and therefore P^{-1} does not exist.

Instead, the choice of L here is as follows (also Fig. 10). Note that the plant P is represented as a delay by 2 stroke steps followed by a down-sampler by 4 stroke steps. Reverting this process, L is chosen as an acausal process with an up-sampler by 4 and then an advance by 2 steps. Furthermore, a digital interpolation filter H is added for a smoother output signal.

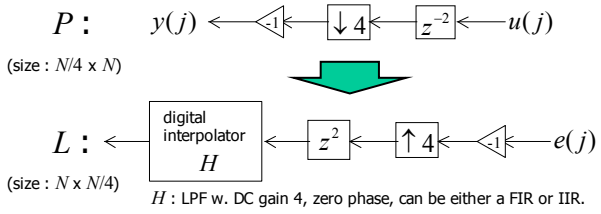

Fig. 10. Learning gain L based on plant P in the ILC for the fuel DOB.

The digital interpolation filter H should be a low pass filter with a DC gain of 4, a cutoff frequency at $\pm\pi/4$, and have zero-phase characteristics (thus acausal). H can be a FIR or an IIR. Fig. 11 shows the concept of digital interpolation.

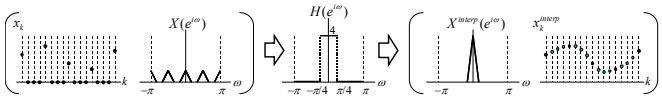

Fig. 11. Digital interpolation $X^{interp}(e^{j\omega}) = H(e^{j\omega})X(e^{j\omega})$.

The above choice of L can actually be regarded as a variant of the pseudo inverse of P. In this case where P is of size $N/4$ x N i.e. "fat", the pseudo inverse of P is $P^*(PP^*)^{-1}$. Then

$$D(z)=z^{-2} \;\Rightarrow\; D^*(1/z^*)=z^2$$

$$\{\downarrow 4\}=\begin{bmatrix}1&0&0&0&0&0&\cdots\\0&0&0&0&1&0&\cdots\\\vdots&&&&&&\ddots\end{bmatrix}\Rightarrow\{\downarrow 4\}^*=\begin{bmatrix}1&0&0&0&0&0&\cdots\\0&0&0&0&1&0&\cdots\\\vdots&&&&&&\ddots\end{bmatrix}^T=\{\uparrow 4\}$$

(size : $N/4$ x N) (size : N x $N/4$)

$$\Rightarrow\begin{cases}P^*=-z^2\{\uparrow 4\}\\ PP^*=I \;\text{ since }\{\downarrow 4\}\{\uparrow 4\}=I\end{cases}\Rightarrow P^*(PP^*)^{-1}=-z^2\{\uparrow 4\}$$

$$\Rightarrow L=HP^*(PP^*)^{-1}=-Hz^2\{\uparrow 4\} \qquad (8)$$

4) Stability and convergence of the ILC scheme

In a general setting of ILC, the stability of the scheme and monotonic convergence of $u(j)$ is evaluated by the maximum singular value of **Q**(**I**-**LP**) i.e. $\bar{\sigma}$ (**Q**(**I**-**LP**)) where **Q**, **L**, and **P** are matrices representing Q, L and P in the lifted domain [6] (see also Appendix). If Q and LP are LTI, one can instead readily evaluate the H_∞ norm $\|Q(I-LP)\|_\infty$. In case of the fuel DOB application, however, this is not possible because LP is not time invariant (LP has a combination of a down-sampler followed by an up-sampler which is not time invariant). However, LP is still linear, hence singular value analysis in the lifted domain representation is still applicable.

A rigorous treatment on singular value analysis of **Q**(**I**-**LP**) is still in progress. It is, however, expected that given the nature of L as a variant of the pseudo inverse of P as stated above, the output of LP should look similar to $u(j)=m_{fi}^{comp}(j)$, the input to LP, as long as $u(j)$ does not have significant components at frequencies higher than $\pi/4$. This indicates that LP should behave effectively like an identity under practical conditions. Therefore, $\bar{\sigma}$ (**Q**(**I**-**LP**)) is expected to be small enough to realize convergence within a few steps.

C. Evaluation by simulation

The proposed ILC scheme is evaluated by simulation. The conditions are similar to what was presented before i.e. air though throttle m_{at} is a measured signal from the actual setup, and the equivalent fuel injection disturbance $\tilde{m}_{fi}$ is a linearly interpolated $\hat{\tilde{m}}_{fi}$ in Fig. 5. These m_{at} and $\tilde{m}_{fi}$ are kept fixed across iterations, whereas $T_{gen}(j)$, $\hat{\tilde{m}}_{fi}(j)$ and $m_{fi}^{comp}(j)$ are observed for each individual iteration.

1) $Q=I$

The simplest ILC structure is when $Q=I$. Fig. 12 shows the results for the 1st and the 2nd iteration. Starting from T_{gen} that deviates from nominal output $G_{Ta}m_{at}$ (same as already shown in Fig. 4), $\hat{\tilde{m}}_{fi}$ and m_{fi}^{comp} are obtained. Fig. 12 shows that m_{fi}^{comp} is an interpolated $\hat{\tilde{m}}_{fi}$ advanced by two steps. When m_{fi}^{comp} from the 1st iteration is applied to the next iteration, T_{gen} now exactly matches the nominal output. Therefore, $\hat{\tilde{m}}_{fi}(j\geq 2)=0$ and iterative learning does not take place any more; in other words, learning has finished (converged) at the 1st iteration with ideal m_{fi}^{comp} obtained and no more updates are necessary.

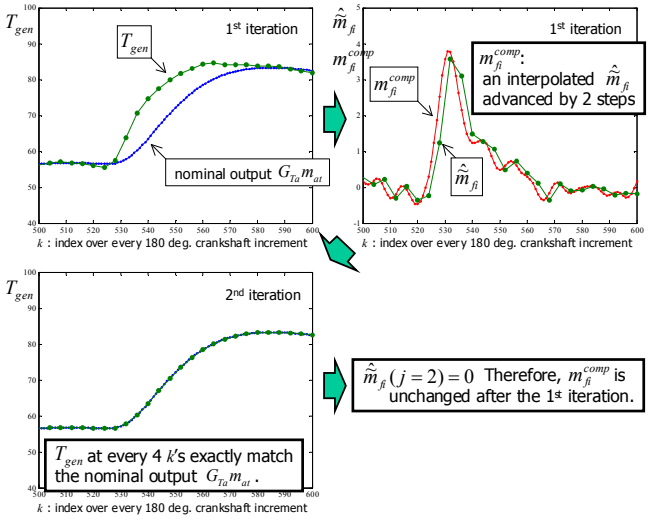

Fig. 12. Simulated ILC results with $Q=I$.

2) LPF-Q with cutoff frequency at $\pi/10$

Here, Q is a zero-phase LPF (thus acausal) with an arbitrarily chosen cutoff frequency at $\pi/10$. m_{fi}^{comp} is different from the previous $Q=I$ case. In Fig. 13, the output torque T_{gen} in the 2nd iteration slightly deviates from the nominal output by a small amount. It is noted that m_{fi}^{comp} in the 2nd iteration is unchanged from the 1st iteration although $\hat{\tilde{m}}_{fi}(j=2)$ is not 0.

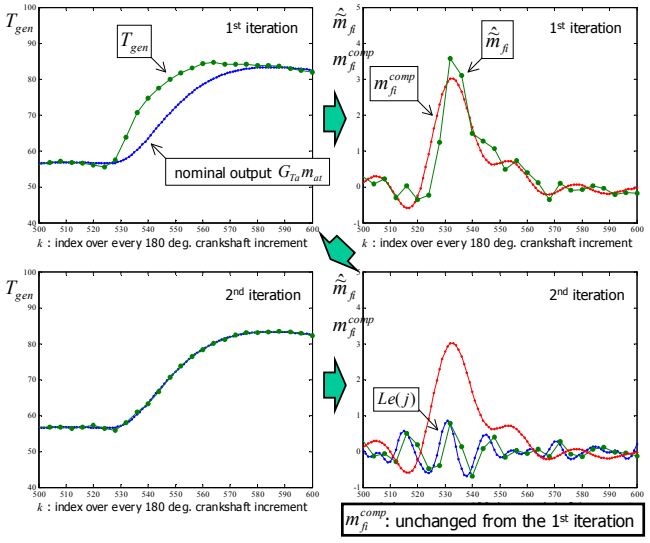

Fig. 13. Simulated ILC results with a LPF-Q.

Above results in the 2nd iteration indicate that the LPF characteristics of the Q filter has eliminated the effect of the non-trivial $\hat{\tilde{m}}_{fi}(j=2)$ having only high frequency components. As a result, iterative learning is converged at the 1st iteration.

3) LPF-Q subjected to torque measurement noise

Torque measurement noise of $N(0,0.1)$ is now assumed in $T_{gen}(j)$ values. Fig. 14 shows $T_{gen}(j)$, $\hat{\tilde{m}}_{fi}(j)$ and $m_{fi}^{comp}(j)$ for up to the 4th iteration. It is shown that m_{fi}^{comp} does not converge any more and now wobbles across iterations. This reflects the downside of ILC schemes in general, i.e. the performance of

ILC is deteriorated when non-repetitive disturbance exists. It is, however, also noted that the wobble is not large and m_{fi}^{comp} keeps its curve similar to what resulted in the previous case (Fig. 13). This is due to the low pass filtering of Q filter. As a result, the output torque T_{gen} stays close to the nominal output from the 2nd iteration and further.

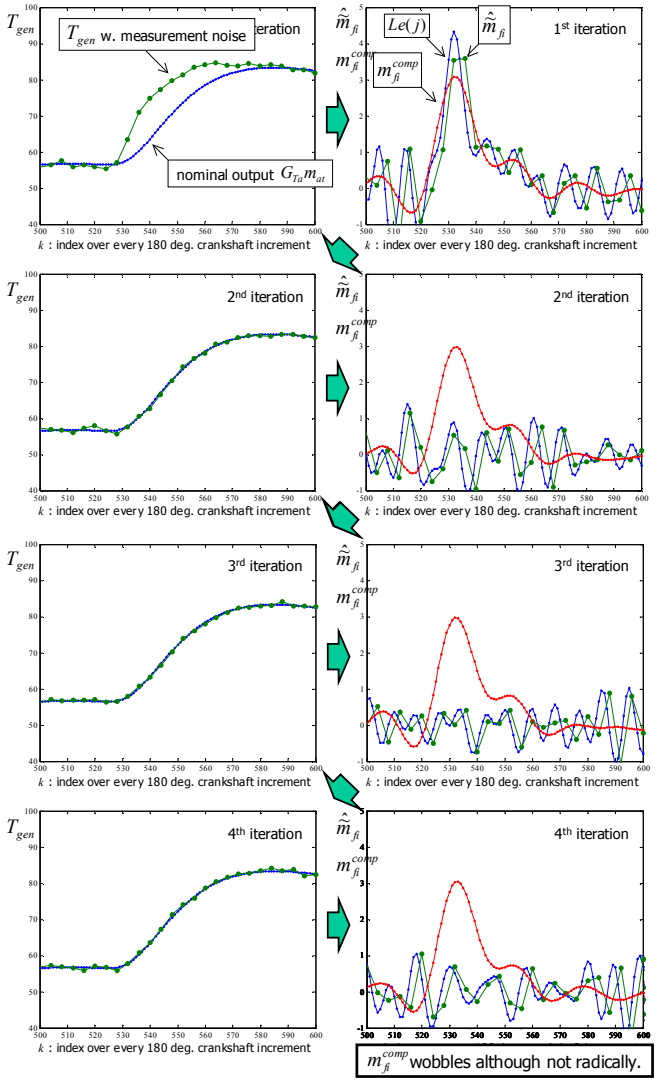

Fig. 14. Simulated ILC results with LPF-Q and torque measurement noise.

IV. Conclusion

The evaluation results of the ILC scheme applied to the fuel DOB problem support the following observations. Iterative learning of disturbance compensation m_{fi}^{comp} from estimated fuel injection disturbance $\hat{\tilde{m}}_{fi}$ is practically converged in a single iteration (i.e. dead-beat learning). This is by virtue of the choice of learning gain L to resemble a plant inverse P^{-1}.

Also, when subjected to non-repetitive measurement noise, m_{fi}^{comp} no longer converges in the strict sense, although results may still be acceptable under practical tolerance conditions. This means that the choice of Q filter should be further investigated since it adjusts rejection of non-repetitive noise.

As for realizing nominal plant performance which is the main objective of this study, significant improvement is shown in model discrepancy detection and compensation compared with the DOB only framework.

Open issues regarding this study include (a) experimental verification of the proposed fuel DOB with ILC, (b) rigorous stability analysis of the ILC scheme, and (c) developing a systematic method for choosing a Q filter for the ILC scheme.

Appendix

In the lifted domain, a linear dynamics $w=G(v)$ from an input $v=\{v_n\}_{n=0}^{N-1}$ to an output $w=\{w_m\}_{m=0}^{M-1}$ is represented as $\underline{w}=\mathbf{G}\underline{v}$ using vertically stacked vectors $\underline{v}=\left[\{v_n\}_{n=0}^{N-1}\right]^T$ and $\underline{w}=\left[\{w_m\}_{m=0}^{M-1}\right]^T$, and a M x N matrix $\mathbf{G}=\{G_{nm}\}_{n,m}$. If G is LTI, $\mathbf{G}$ is made from the unit pulse response of G i.e. $\{g_k\}_{k=-\infty}^{\infty}$ with reversed order, shifted, and stacked vertically as

$$\mathbf{G}=\begin{bmatrix}\{g_k\}_{k=0}^{-N+1}\\ \{g_k\}_{k=1}^{-N+2}\\ \vdots\\ \{g_k\}_{k=M-1}^{-N+M}\end{bmatrix}=\begin{bmatrix}g_0 & g_{-1} & \cdots & g_{-N+1}\\ g_1 & g_0 & \cdots & g_{-N+2}\\ \vdots & \vdots & & \vdots\\ g_{M-1} & g_{M-2} & \cdots & g_{-N+M}\end{bmatrix} \tag{9}$$

If G is LTI and also $M = N$ in above, then $\mathbf{G}$ becomes a Toeplitz matrix. If G is not time invariant but still linear, there still exists a $\mathbf{G}$, however, it is no longer Toeplitz. For instance, $LP=HP^*(PP^*)^{-1}P=Hz^2\{\uparrow 4\}\{\downarrow 4\}z^{-2}$ with a zero-phase LPF-H has the following lifted domain representation

$$\mathbf{LP}=\begin{bmatrix}h_0 & h_1 & h_2 & \cdots\\ h_1 & h_0 & h_1 & \cdots\\ h_2 & h_1 & h_0 & \cdots\\ \vdots & \vdots & \vdots & \ddots\end{bmatrix}\begin{bmatrix}0 & & & & & & & \\ & 0 & & & & & 0 & \\ & & 1 & & & & & \\ & & & 0 & & & & \\ & & & & 0 & & & \\ & & & & & 1 & & \\ & 0 & & & & & 0 & \\ & & & & & & & \ddots\end{bmatrix}=\begin{bmatrix}0 & 0 & h_2 & 0 & 0 & 0 & h_6 & 0 & \cdots\\ 0 & 0 & h_1 & 0 & 0 & 0 & h_5 & 0 & \cdots\\ 0 & 0 & h_0 & 0 & 0 & 0 & h_4 & 0 & \cdots\\ 0 & 0 & h_1 & 0 & 0 & 0 & h_3 & 0 & \cdots\\ 0 & 0 & h_2 & 0 & 0 & 0 & h_2 & 0 & \cdots\\ 0 & 0 & h_3 & 0 & 0 & 0 & h_1 & 0 & \cdots\\ 0 & 0 & h_4 & 0 & 0 & 0 & h_0 & 0 & \cdots\\ 0 & 0 & h_5 & 0 & 0 & 0 & h_1 & 0 & \cdots\\ \vdots & \vdots & \vdots & \vdots & \vdots & \vdots & \vdots & \vdots & \ddots\end{bmatrix} \tag{10}$$

where h_k's represent the unit pulse response of H.

References

[1] T. Nagata, H. Hur, and M. Tomizuka, "Model-based control for smooth gear shifting by engine-AT collaboration", Proceedings of the 8th International Symposium on Advanced Vehicle Control (AVEC '06), pp. 635-640, Taiwan, 2006.

[2] O. Ulrich, R. Wlodarczyk, and M.T. Wlodarczyk, "High-accuracy low-cost cylinder pressure sensor for advanced engine controls", Journal of Engines, 2001-01-0991, SAE. 2001.

[3] L. Guzzella, and C.H. Onder, *Introduction to Modeling and Control of Internal Combustion Engine Systems*, Springer-Verlag, New York, 2004.

[4] T. Nagata, and M. Tomizuka, "Robust engine torque control by discrete event disturbance observer", Proceedings of the IFAC World Congress (IFAC WC 2008), pp. 9473-9478, Seoul, Korea, 2008.

[5] T. Nagata, and M. Tomizuka, "Engine torque control based on discrete event model and disturbance observer", Proceedings of the ASME Int. Mech. Eng. Congr. Expo. (IMECE2007), IMECE2007-41439, Seattle, Washington, 2007.

[6] D.A. Bristow, M. Tharayil, and A.G. Alleyne, "A Survey of Iterative Learning Control: A learning-based method for high-performance tracking control", IEEE control systems magazine, Vol. 26, pp. 96-114, 2006.